Electronic Structure of the Creutz-Taube Ion

Li-Tai Zhang,[†] Jaeju Ko,[†] and Mary Jo Ondrechen*[‡]

Contribution from the Department of Chemistry, Northeastern University, Boston, Massachusetts 02115, and Kermisk Institut, Aarhus Universitet, DK-8000 Aarhus C, Denmark.
Received August 15, 1986

Abstract: An electronic structure calculation on the Creutz-Taube ion, a pyrazine-bridged mixed-valence dimer of ruthenium, by the Hartree-Fock-Slater discrete variational method is reported. The calculation is performed once by using the symmetric crystallographic geometry and again by using a plausible asymmetric geometry. The converged ground states in the two geometries are very similar and both exhibit strong mixing of the two Ru $4d_{xz}$ orbitals with one π^* orbital on the pyrazine bridging ligand. The unpaired spin is shared equally by the two metal ions. The present results constitute evidence for a delocalized ground state. Electronic transition energies were calculated utilizing a transition operator (TO) method. Assignment based on the TO results are made for almost all of the transitions observed to date by optical absorption or MCD. The two Ru $4d_{xz}$ orbitals and one pyrazine π^* orbital form linear combinations which we label as bonding (B), nonbonding (N), and antibonding (A) combinations. The low-energy MCD features observed at 2000 and 4000 cm^{-1} we tentatively assign to particular $t_{2g} \rightarrow N$ transitions. The intervalence transfer (IT) band at 6400 cm^{-1} is better described as a bonding-to-nonbonding transition and therefore has both IT and π^*-to-metal charge-transfer character. The features in the range 17 000-20 000 cm^{-1} are assigned to particular $t_{2g} \rightarrow A$ transitions. The assignment of the band at 39 700 cm^{-1} to a $\pi \rightarrow \pi^*$ transition is confirmed. A method for obtaining model Hamiltonian parameters for the calculation of the optical absorption line shape from the TO results is presented. This method gives only the purely electronic part of the model Hamiltonian. We also present a method for the calculation of the parameters in an expanded purely electronic model Hamiltonian designed to calculate the components of the (anisotropic) EPR g tensor. This latter method utilizes the ground-state results of the present calculation.

I. Introduction

Major strides in the field of inorganic synthesis in the last 20 years have produced a multitude of new mixed valence compounds, bimetallic species, and backboned complexes.[1] Studies of these compounds have raised important questions regarding electron delocalization, rates of electron transfer, and the manifestations of electronic structure and dynamics in optical absorption (OA), EPR, and MCD spectra. Bridged mixed-valence and bimetallic species, in which two metal ions are connected by some bridging ligand, have been the center of especially intense attention recently.[1] Perhaps the best known of these bridged species is the Creutz-Taube (C-T) ion,[2-13] a pyrazine-bridged mixed-valence dimer of ruthenium

In a mixed-valence complex such as the C-T ion, the ground state may be either delocalized (with two classical structures in resonance) or localized (with two classical structures in equilibrium and with observable metal-to-metal electron transfer). The nature of the ground state of the C-T ion has been a matter of intense controversy.[2-13] The purpose of the present paper is to report new electronic structure calculations on the Creutz-Taube ion by using two different plausible geometries, one symmetric and one asymmetric.

In an earlier note Ondrechen, Ellis, and Ratner (OER)[14] reported on a preliminary electronic structure calculation on the Creutz-Taube ion by using the symmetric crystallographic geometry of Beattie et al.[5] The OER results showed strong mixing of the two Ru $4d_{xz}$ orbitals (one on each side) with one π^* orbital on the pyrazine bridge represented by this view from above as

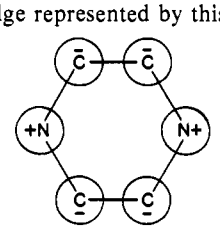

The two Ru ions were reported to be nearly identical and strongly coupled via the bridging ligand. This suggests a delocalized or valence-averaged ground state. However, one could argue that the results of the MO calculation are geometry-dependent and that the two Ru ions were found to be nearly identical and strongly mixed with a π^* orbital because a symmetric geometry was assumed. It is possible that the MO calculation could show localized behavior if a plausible asymmetric geometric is assumed.

The aims of the present paper are as follows: (1) to report and compare the results of two MO calculations, one on the Creutz-Taube ion by using the symmetric crystallographic geometry of Ludi et al.[7] and the other by using a plausible asymmetric geometry based on the crystal structures of the corresponding 4+ (Ru^{II}···Ru^{II}) and 6+ (Ru^{III}···Ru^{III}) ions; (2) to report detailed transition operator calculations (not included in the earlier note[14]) on the 5+ C-T ion; (3) to make assignments of observed electronic transitions, especially of some experimental MCD results[9,13] which have appeared since the publication of the OER note; (4) to present the details of the calculation of the components of the EPR g tensor based on a model advanced by us in a recent communication;[15] and (5) to show how to use the present transition

[†] Northeastern University.
[‡] On sabbatical leave at Aarhus Universitet Oct 1986-June 1987. Permanent address: Northeastern University.

(1) (a) Creutz, C. *Prog. Inorg. Chem.* **1983**, *30*, 1-73. (b) Endicott, J. F.; Kumar, K.; Ramasami, T.; Rotzinger, F. P. *Ibid.* **1983**, *30*, 141-187. (c) Haim, A. *Ibid.* **1983**, *30*, 273-357. (d) Meyer, T. J. *Ibid.* **1983**, *30*, 389-440. (e) Sutin, N. *Ibid.* **1983**, *30*, 441-498.
(2) Creutz, C.; Taube, H. *J. Am. Chem. Soc.* **1969**, *91*, 3988.
(3) Creutz, C.; Taube, H. *Ibid.* **1973**, 1086-1094.
(4) Beattie, J. K.; Hush, N. S.; Taylor, P. R. *Inorg. Chem.* **1976**, *15*, 992-993.
(5) Beattie, J. K.; Hush, N. S.; Taylor, P. R.; Raston, C. L.; White, A. H. *J. Chem. Soc., Dalton Trans.* **1977**, 1121-1124.
(6) Piepho, S. B.; Krausz, E. R.; Schatz, P. N. *J. Am. Chem. Soc.* **1978**, *100*, 2296-3005.
(7) Fürholz, U.; Bürgi, H.-B.; Wagner, F. E.; Stebler, A.; Ammeter, J. H.; Krausz, E.; Clark, R. J. H.; Stead, M. J.; Ludi, A. *J. Am. Chem. Soc.* **1984**, *106*, 121-123.
(8) Stebler, A.; Ammeter, J. H.; Fürholz, U.; Ludi, A. *Inorg. Chem.* **1984**, *23*, 2764-2767.
(9) Krausz, E.; Ludi, A. *Inorg. Chem.* **1985**, *24*, 939-943.
(10) Fürholz, U.; Joss, S.; Bürgi, H.-B.; Ludi, A. *Inorg. Chem.* **1985**, *24*, 943-948.
(11) Joss, S.; Bürgi, H.-B.; Ludi, A. *Inorg. Chem.* **1985**, *24*, 949-954.
(12) Dubicki, L.; Ferguson, J.; Krausz, E. R. *J. Am. Chem. Soc.* **1985**, *107*, 179-182.
(13) (a) Krausz, E. R. *Chem. Phys. Lett.* **1985**, *120*, 113-117. (b) Krausz, E. R.; Mau, A. W. H. *Inorg. Chem.* **1986**, *25*, 1484-1488.
(14) Ondrechen, M. J.; Ellis, D. E.; Ratner, M. A. *Chem. Phys. Lett.* **1984**, *109*, 50-55.

0002-7863/87/1509-1666$01.50/0

operator results to obtain the parameters in the purely electronic part of a model Hamiltonian for predicting OA line shapes[16,17] for compounds like the C–T ion.

In the following section, we outline briefly our method for the calculation of the electronic structure. Section III gives the input data, including geometries, used in the present calculation. Results for the ground states in the symmetric and asymmetric geometries are then presented and compared. Transition-state results are presented in section V. Then, the use of the transition-state results in the OA line shape problem is discussed. In section VII, the calculation of the components of the EPR g tensor is discussed. In the subsequent section, some further thoughts are given on the assignment of electronic transitions based on the transition-state results, plus the probable effects of spin-orbit coupling. We conclude with section IX.

II. A Brief Outline of the Electronic Structure Method[18-20]

The Hartree–Fock–Slater discrete variational method (HFS–DVM) has been applied extensively to both molecules and solids. The DVM is one method for solving the HFS equations without invoking the muffin-tin approximation. It is a first-principles, nonempirical SCF method.

We utilize the spin-polarized one-electron local density model, the Hamiltonian for which is given by

$$\hat{h}_\mu = \hat{T} + \hat{V}_c + \hat{V}_{x,\mu} \tag{1}$$

where μ is a spin index ($\uparrow$ or $\downarrow$), $\hat{T}$ and $\hat{V}_c$ are the kinetic energy and Coulomb potential operators, and $\hat{V}_{x,\mu}$ is the exchange and correlation potential for an electron with spin μ, given by

$$\hat{V}_{x,\mu} = -3X_\alpha(3\rho_\mu/4\pi)^{1/3} \tag{2}$$

where X_α is a scaling constant, with $^2/_3 < x_\alpha < 1$. The exchange-correlation potential depends on the spin density ρ_μ, which is taken to be a linear combination of single particle contributions

$$\rho_\mu(r) = \sum_n f_{n\mu}|\psi_{n\mu}(r)|^2 \tag{3}$$

Here f_n is an occupation number and $\psi_{n\mu}$ is an eigenfunction of $\hat{h}_\mu$. This scheme (eq 1–3) is solved self-consistently. The molecular wave functions are expanded in the usual LCAO fashion

$$\psi_{n\mu} = \sum_j C_{n\mu j}\phi_j \tag{4}$$

where the ϕ_j's are symmetry-adapted linear combinations of atomic orbitals. The atomic orbitals (AO's) are obtained numerically by using an HFS-SCF procedure on the atoms. The elements of the Hamiltonian and overlap matrices are obtained by direct numerical integration, employing a diophantine integration method.[21]

III. Details of the Calculation

For the present calculations on the C–T ion, we take $X_\alpha = 0.7$.[20] An all-electron valence basis (1s on H; 1s, 2s, 2p on C; 1s, 2s, 2p on N; 1s–6s, 2p–5p, 3d–4d on Ru) is used, with the core functions (1s on C; 1s on N; 1s–3s, 2p–3p, 3d on Ru) frozen throughout the iterations.

The ground-state calculation is performed twice, once by using a symmetric geometry and again by using an asymmetric geometry. The earlier OER calculation used the 1977 crystallographic data of Beattie et al.[5] on a mixed bromide chloride salt of the C–T ion. For the present work, we decided to use the 1984 data of Ludi et al.[7] on the chloride pentahydrate (C–T)$Cl_5 \cdot 5H_2O$, because Ludi et al. also reported crystallographic data on the corresponding 4+ (Ru^{II}···Ru^{II}) and 6+ (Ru^{III}···Ru^{III}) dimers. From the geometries of the 4+ and 6+ ions we can infer a plausible asymmetric geometry for the 5+ ion.

Table I. Internuclear Distances (Å)[7]

	symmetric geometry both Ru ions	asymmetric geometry	
		Ru(II)	Ru(III)
Ru–N (pyz)	2.002	2.01	2.12
Ru–N (cis)	2.110	2.13	2.10
Ru–N (trans)	2.135	2.15	2.09

Table II. Molecular Spin-Orbital Energies and Symmetries[a]

spin orbital (in C_s)	energy (eV) symmetric geometry	energy (eV) asymmetric geometry	symmetry (in D_{2h})[b]	symmetry (in C_{2v})[c]
42A′–	−19.2368	−19.2988	B_{3u}	A_1
42A′+	−19.3452	−19.3964	B_{3u}	A_1
41A′–	−20.7065	−20.7065	B_{2g}	B_1
40A′–	−20.7515	−20.7162	B_{1u}, A_g	B_1, A_1
39A′–	−20.8244	−20.8086		
28A″–	−20.8519	−20.8216	B_{3g}, B_{2u}	A_2, B_2
27A″–	−20.9783	−20.9358		
41A′+	−21.0774	−21.0856	B_{2g}	B_1
40A′+	−21.1609	−21.0992	B_{1u}, A_g	B_1, A_1
39A′+	−21.2001	−21.2201		
28A″+	−21.2602	−21.2037	B_{3g}, B_{2u}	A_2, B_2
27A″+	−21.3483	−21.3427		
38A′–	−21.5307	−21.3955	B_{3u}	A_1
38A′+	−21.7907	−21.6694	B_{3u}	A_1

[a] Spin orbitals below the dashed line are occupied; those above are unoccupied. [b] Ammonia H atoms excluded. [c] Ammonia H atoms included.

The structures of the 5+ ion reported in ref 5 and 7 are nearly identical; however, there are some small differences. Both references found the two Ru atoms to be equivalent with well-refined Ru–N bond distances, which suggests a symmetric (delocalized) ground state. Both show significant shortening of the Ru–N(pyz) bond relative to the Ru–NH_3 bond lengths. The Ru–N(pyz), Ru–N(cis), and Ru–N(trans) bond distances were reported to be 2.006, 2.110, and 2.127 Å, respectively, in ref 5 and 2.002, 2.110, and 2.135 Å, respectively, in ref 7. Thus, the trans effect observed in ref 7 is a little bit larger than that observed in ref 5. Because of these small but possibly significant differences in the Ru–N bond distances, we decided to repeat the OER electronic structure calculation, this time by using the symmetric geometry of ref 7. We then perform the calculation again on the 5+ (C–T) ion in an asymmetric geometry, by using the Ru–N bond distances reported[7] for the 4+ (Ru^{II}–Ru^{II}) ion on one side of the molecule and the Ru–N bond distances reported for the 6+ (Ru^{III}–Ru^{III}) ion on the other side of the molecule. This asymmetric geometry is a plausible geometry for the ground state of the 5+ C–T ion if it is a localized species (i.e., with two classical structures in equilibrium and not in resonance).[25]

The purpose of the calculation on the asymmetric geometry is to see if bias was introduced into the calculation which used the symmetric crystallographic geometry. It is not our intent to gain potential energy surface information from comparison of the

(15) Ko, J.; Zhang, L.-T.; Ondrechen, M. J. *J. Am. Chem. Soc.* **1986**, *108*, 1712–1713.
(16) Root, L. J.; Ondrechen, M. J. *Chem. Phys. Lett.* **1982**, *93*, 421–424.
(17) Ko, J.; Ondrechen, M. J. *J. Am. Chem. Soc.* **1985**, *107*, 6161–6167.
(18) Delley, B.; Ellis, D. E. *J. Chem. Phys.* **1972**, *16*, 1949 and references cited therein.
(19) Rosén, A.; Ellis, D. E.; Adachi, H.; Averill, F. W. *J. Chem. Phys.* **1976**, *65*, 3629–3634.
(20) Baerends, E. J.; Ros, P. *Int. J. Quantum Chem. Symp.* **1978**, *12*, 169.
(21) Ellis, D. E. *Int. J. Quantum Chem.* **1968**, *IIS*, 35–42.
(22) Ondrechen, M. J.; Ko, J.; Zhang, L.-T., the following paper in this issue.
(23) Slater, J. C. *Adv. Quantum Chem.* **1972**, *6*, 1.
(24) Neuenschwander, K.; Piepho, S. B.; Schatz, P. N. *J. Am. Chem. Soc.* **1985**, *107*, 7862–7869.
(25) Another possible way to construct an asymmetric geometry is to use the bond distances of the monomers $[(NH_3)_5Ru(pyz)]^{2+/3+}$. However the difference in Ru–pyz bond distances in the 2+ and 3+ monomers is only 0.07 Å. This difference is greater between the (II,II) and (III,III) dimers (0.10 Å). Therefore, we chose the dimer bond distances to construct an asymmetric geometry because they were probably more likely to show localization behavior.

Table III. Basis Set Expansion Coefficients for Some Important Spin Orbitals

	symmetric geometry					
	$4d_{xz}$		$2P_x$			
	Ru(1)	Ru(2)	$C_3 + C_4$	$C_5 + C_6$	N^7_{pyz}	N^8_{pyz}
38A′+	0.566	−0.599	−0.455	−0.432	0.300	0.288
41A′+	0.693	0.687	−0.303	0.253	−0.080	0.111
42A′+	0.406	−0.389	0.646	0.603	−0.655	−0.638
33A′+	−0.118	−0.108	−0.449	0.368	0.555	0.509
29A′+	0.051	−0.062	0.482	0.521	0.324	0.408
38A′−	0.525	−0.573	−0.501	−0.481	0.354	0.338
41A′−	0.693	0.678	−0.319	0.246	−0.054	0.107
42A′−	0.459	−0.428	0.607	0.573	−0.626	−0.610
33A′−	−0.107	−0.098	−0.450	0.368	−0.560	0.513
29A′−	0.047	−0.058	0.480	0.520	0.326	0.411

39A′+	−0.987	$d_{x^2-y^2}$ on Ru(2)	39A′−	−0.986	$d_{x^2-y^2}$ on Ru(2)
40A′+	−1.00	$d_{x^2-y^2}$ on Ru(1)	40A′−	−1.001	$d_{x^2-y^2}$ on Ru(1)
27A″+	0.996	d_{yz} on Ru(2)	27A″−	0.997	d_{yz} on Ru(2)
28A″+	−0.986	d_{yz} on Ru(1)	28A″−	−0.987	d_{yz} on Ru(1)

electronic structures in the symmetric and asymmetric geometries; the total energy is one property which cannot be calculated with accuracy by the HFS-DVM. The problem of the potential energy surfaces is addressed by us in the next paper.[22]

Internuclear distances used in the calculations are summarized in Table I.

For improvement of the basis set AO's, the HFS-DVM molecular calculation was converged, then the resulting Mulliken populations were used to calculate better atomic basis functions.[19] This process was repeated a few times to obtain a high quality basis set. The basis set used in the present work was close to but slightly more refined than that of OER.[14]

The NH_3 groups are rotated so that the ion has a plane of symmetry: a plane *containing* the metal–metal axis. C_s is the highest symmetry which can be assumed a priori for the C–T ion in this type of electronic structure calculation.

IV. Ground-State Results

Molecular orbital energies and symmetries for the spin orbitals near the HOMO–LUMO gap are given in Table II. Energies (in eV) are given for the converged ground states of the C–T ion in the symmetric and asymmetric geometries. The symmetry is given for each MO in D_{2h} (the symmetry of the ion if the H atoms on the NH_3 groups are ignored), C_{2v} (the symmetry if the H atoms on NH_3 are not ignored), and C_s (the symmetry used in the calculation, which presumes that the two Ru ions are inequivalent). A′ and A″ designate the two irreducible representations in the point group C_s. In C_s, the spin state is designated by + or −. Since Koopmans' theorem is not obeyed in the local density model, we regard as significant the energy *differences* between the converged ground-state spin orbitals; the absolute energies are less meaningful. Therefore, in order to compare the present results for the symmetric and asymmetric geometries, we have added a constant equal to −0.1246 eV to each of the energy eigenvalues for the asymmetric geometry, so that the energies of their respective lowest unoccupied molecular spin orbitals (LUMSO's) coincide. It is apparent from Table II that the energy gaps between spin orbitals in the symmetric geometry are very similar to those for corresponding spin orbitals in the asymmetric geometry. (Differences between symmetric and asymmetric energies are approximately 0.1 eV.) Furthermore, since the present calculation is spin-polarized, energies for the + spin orbitals are different from those of the corresponding − spin orbitals.

Figure 1 shows the energy level diagram for the converged ground state of (1) the previous OER calculation, (2) the present symmetric geometry, and (3) the present asymmetric geometry. Again, a constant equal to −0.1246 eV has been added to all of the energy eigenvalues for the asymmetric case, and a constant equal to −0.1865 eV has been added to all of the OER energy eigenvalues, so that the energies of all three LUMSO's coincide. (This shifting of the energy origin is a consequence of the properties of the local density model.) A dotted line in Figure 1 designates the LUMSO. The spin orbitals close in energy to the

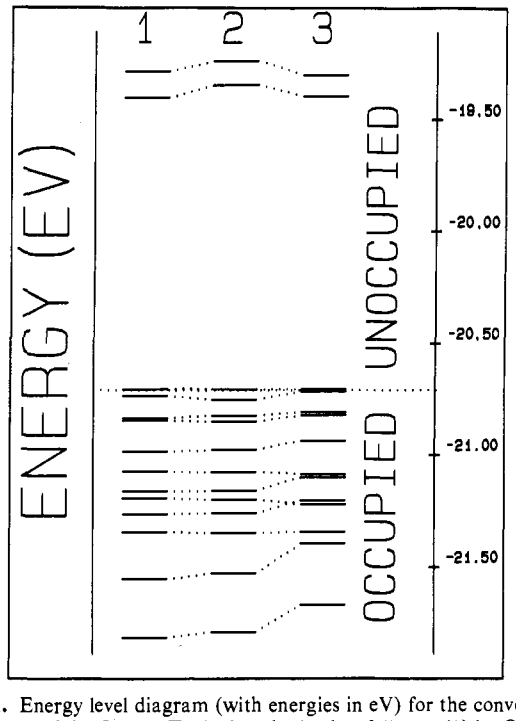

Figure 1. Energy level diagram (with energies in eV) for the converged ground state of the Creutz–Taube ion obtained as follows: (1) by OER[14] using the symmetric geometry of Beattie et al.,[5] (2) in the present calculation using the symmetric geometry of Ludi et al.,[7] and (3) in the present calculation using a plausible asymmetric geometry based on crystallograpohic data for the corresponding (II,II) and (III,III) ions.

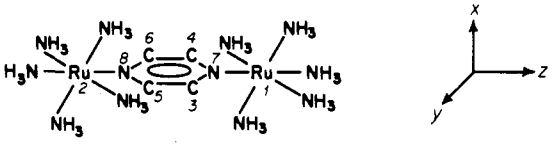

Figure 2. The Creutz–Taube ion, with the atom numbering scheme used in the present calculation.

LUMSO are all occupied; the next lowest unoccupied orbitals are about 1.4 eV higher in energy than the LUMSO.

One notes that some of the energy levels of our present symmetric calculation differ slightly but significantly from those of the previous OER calculation. This we attribute to the slight differences in Ru–N bond lengths in these two symmetric geometries (vide Supra). Likewise, the small differences in the relative MO energies between the present symmetric and asymmetric geometries result from the differences in bond lengths.

The basis set expansion coefficients of the converged ground states with symmetric and asymmetric geometries are given in Tables III and IV, respectively. Figure 2 shows the atom num-

Table IV. Basis Set Expansion Coefficients for Some Important Spin Orbitals

	asymmetric geometry					
	$4d_{xz}$		$2P_x$			
	Ru(1)	Ru(2)	$C_3 + C_4$	$C_5 + C_6$	N^7_{pyz}	N^8_{pyz}
38A′+	0.576	−0.616	−0.458	−0.373	0.277	0.287
41A′+	−0.659	−0.691	0.314	−0.182	0.037	−0.133
42A′+	0.430	−0.320	0.647	0.623	−0.666	−0.636
33A′+	0.114	0.091	0.407	−0.426	0.541	−0.522
29A′+	−0.055	0.046	−0.517	−0.504	−0.358	−0.360
38A′−	0.567	−0.553	−0.525	−0.416	0.335	0.347
41A′−	−0.618	−0.711	0.297	−0.195	0.030	−0.109
42A′−	0.487	−0.364	0.602	0.595	−0.636	−0.608
33A′−	0.104	0.082	0.408	−0.427	0.546	−0.527
29A′−	−0.051	0.042	−0.516	−0.502	−0.360	−0.363

39A′+	0.986	$d_{x^2-y^2}$ on Ru(2)	39A′−	0.984	$d_{x^2-y^2}$ on Ru(2)
40A′+	0.986	$d_{x^2-y^2}$ on Ru(1)	40A′−	0.971	$d_{x^2-y^2}$ on Ru(1)
27A″+	0.999	d_{yz} on Ru(2)	27A″−	0.997	d_{yz} on Ru(2)
28A″+	−0.988	d_{yz} on Ru(1)	28A″−	−0.986	d_{yz} on Ru(1)

Table V. Total Valence Population

	symmetric geometry		asymmetric geometry	
subshell	Ru(1)	Ru(2)	Ru(1)	Ru(2)
4s	1.97	1.97	1.97	1.97
4p	5.96	5.96	5.96	5.96
4d	6.24	6.22	6.25	6.23
5s	0.07	0.08	0.07	0.09
5p	0.20	0.21	0.19	0.21
6s	0.04	0.02	0.03	0.02

bering scheme. Notice in Table III that for the symmetric geometric, the coefficients for $4d_{xz}$ on Ru(1) and on Ru(2) are very close to each other in each spin orbital. The MO's 38A′, 41A′, and 42A′ are bonding, nonbonding, and antibonding combinations of π^* and the two Ru $4d_{xz}$ orbitals and are shown schematically in Figure 3. The nonbonding 41A′ orbital also contains a small amount of another π^* orbital. (Note that the occupation of this other π^* orbital in 41A′ is proportional to the sum of the squares of the coefficients and is relatively small.) Also notice that the nonbonding combination of $4d_{xz}$ orbitals is slightly higher in energy than the $d_{x^2-y^2}$ and d_{yz} orbitals, while the bonding combination is significantly lower in energy due to the mixing with the pyrazine π^* orbital.

From comparison of Tables III and IV, one sees that the basis set expansion coefficients for the symmetric and asymmetric geometries are similar. In the asymmetric geometry, there is still substantial mixing of the Ru $4d_{xz}$ orbitals on the two sides via the π^* orbital depicted above.

Mulliken populations for Ru(1) and Ru(2) for the symmetric and asymmetric geometries are given in Table V. Again in each geometry Ru(1) and Ru(2) are nearly identical, and the results for the two geometries are very close.

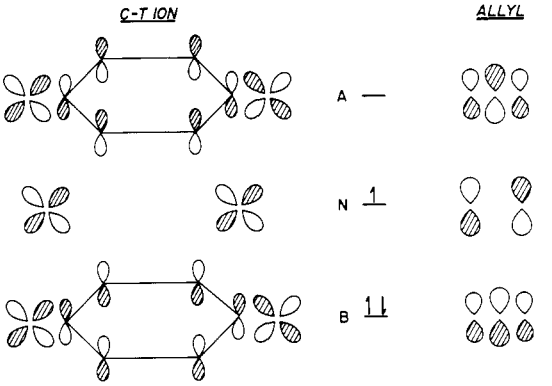

Figure 3. A schematic diagram of the three MO's containing the Ru $4d_{xz}$ basis functions, with their occupations. Analogy to the three Hückel MO's of the allyl radical is noted.

V. Transition-State Results

In the HFS-DVM, the energies of the optical transitions cannot be obtained with accuracy from simple subtraction of two ground-state MO energies. Transition energies are properties of both initial and final electronic states. These energies were obtained by using a transition operator method.[23]

Table VI compares the experimental OA and MCD transition energies with those obtained from our transition operator calculations. In the center of Table VI, we report the transition frequency, the assignment, and the polarization.

Table VI. Comparison of Transition Energies[a]

experimental				transition operator			simple seven state model[b]		
λ (nm)	ν (cm^{-1})	assignment	ref	ν (cm^{-1})	assignment	pol.	ν (cm^{-1})	assignment	pol.
252	39 700	$\pi \rightarrow \pi^*$	3	42 800	$\pi \rightarrow \pi^*$	z			
270 sh	37 000 sh	OA	3	40 400	$\pi \rightarrow A$	sf			
				37 700	$B \rightarrow e_g$	x			
				33 500	$t_{2g} \rightarrow e_g$[a]	x, y, z			
490	20 400	MCD	9	21 200	$t_{2g} \rightarrow A$	x	17 000	$4d_{yz} \rightarrow A^1$	x
565	17 700	$t_{2g} \rightarrow \pi^*$	2	19 000	$N \rightarrow A$	z	17 000[w]	$4d_{yz} \rightarrow A^s$	z
575	17 400	MCD	9				16 000[w]	$4d_{x^2-y^2} \rightarrow A^s$	z
							16 000	$4d_{x^2-y^2} \rightarrow A^1$	x
							15 000	$N \rightarrow A$	z
781	12 800	MCD	9						
850 sh	12 000 sh	OA	3						
1570	6370	IT	2	6 600	IT ($B \rightarrow N$)	z	5 700	$B \rightarrow N$	z
2500	4 000	MCD	13	2 900	$t_{2g} \rightarrow N$	sf	2 300	$4d_{yz} \rightarrow N$	$x + y$
5000	2 000	MCD	13	2 260	$t_{2g} \rightarrow N$	x	1 500	$4d_{x^2-y^2} \rightarrow N$	$x + y$

[a] w = weak; l = a major component; s = a minor component; sf = symmetry forbidden; sh = shoulder; a = multiple transitions at same frequency; B = bonding combination of Ru(1) $4d_{xz}$, π^* and Ru(2) $4d_{xz}$; N = nonbonding combination of Ru(1) $4d_{xz}$, π^* and Ru(2) $4d_{xz}$; A = antibonding combination of Ru(1) $4d_{xz}$, π^* and Ru(2) $4d_{xz}$. [b] Equations 6–10.

The transition observed in the absorption spectrum at 39 700 cm^{-1} was previously assigned to $\pi \rightarrow \pi^*$.[3] We find a z-polarized transition at 42 800 cm^{-1}. Upon examination of the eigenfunctions we find that this is a $\pi \rightarrow \pi^*$ transition on the pyrazine ring, consistent with the original assignment. Reference 3 also reported a weak shoulder at 37 000 cm^{-1}. Since this is just a shoulder and the position of its origin therefore carries a higher degree of uncertainty than does a well-resolved single absorption band, we cannot make an assignment with confidence. However, we can suggest three possibilities: (1) a symmetry forbidden π-to-antibonding transition which we predict would occur at 40 400 cm^{-1}, (2) an x-polarized bonding-to-e_g transition at 37 700 cm^{-1} or, (3) a set of $t_{2g} \rightarrow e_g$ transitions at about 33 500 cm^{-1} which are Laporte forbidden for the exactly octahedral metal ion but are formally allowed (but probably not very strong) in the pyrazine-bridged complex.

There is a strong, broad absorption band with maximum at 17 700 cm^{-1} which has been assigned to $t_{2g} \rightarrow \pi^*$. This band contains multiple components, including the z-polarized nonbonding-to-antibonding transition (predicted at 19 000 cm^{-1}) plus uncoupled (i.e., not d_{xz}) t_{2g}-to-antibonding (predicted at 21 200 cm^{-1}, x-polarized). The two MCD features at 20 400 and 17 400 cm^{-1} may be components of the $t_{2g} \rightarrow A$ band; this will be dealt with in greater detail in section VIII.

The transition operator technique was able to account for neither the observed MCD feature at 12 800 cm^{-1} nor the shoulder in the OA spectrum at about 12 000 cm^{-1}.

The IT band, which is z-polarized with maximum at about 6400 cm^{-1}, was predicted to have origin at about 6600 cm^{-1}. We prefer to call this transition bonding-to-nonbonding, because it contains both IT character and π^*-to-metal charge-transfer character.

The low-energy MCD transitions observed[13] at approximately 4000 and 2000 cm^{-1} are more difficult to assign with the transition operator method alone. Clearly, at the low end of the energy spectrum, percent errors will be relatively high. (In this energy range, the errors in the transition operator method are probably of order 1000 cm^{-1}.) In addition, the calculated transition energies from the nonrelativistic HFS-DVM do not contain spin-orbit coupling effects (also of order 1000 cm^{-1}) (see section VIII).

VI. The OA Line Shape Problem—How To Obtain Model Hamiltonian Parameters

To calculate the OA line shape of the IT (bonding-to-nonbonding) and of the nonbonding-to-antibonding transitions in bridged mixed-valence dimers, we have developed a vibronic coupling model.[16,17,22] The model contains a purely electronic term, a purely nuclear term $\hat{H}_v$, and a vibronic coupling term $\hat{H}_{e-v}$, with the Hamiltonian given by

$$\hat{H} = \hat{H}_e + \hat{H}_v + \hat{H}_{e-v} \tag{5}$$

The calculation of the parameters contained in $\hat{H}_v$ and $\hat{H}_{e-v}$ do not involve our electronic structure calculation and will be discussed in the next paper.[22]

The purely electronic term is given by

$$\hat{H}_e = J(a_1^+a_2 + a_2^+a_3 + a_2^+a_1 + a_3^+a_2) + \alpha a_2^+a_2 \tag{6}$$

Here a_i^+ and a_i are the creation and annihilation operators for the ith electronic state. Sites 1 and 3 are the parent metal states, assumed to be degenerate, and site 2 is the parent bridge state, whose energy is different by α from that of the metal basis states. In the case of the C–T ion, sites 1, 2, and 3 are the Ru $4d_{xz}$ (left), the coupled π^* and the Ru $4d_{xz}$ (right) orbitals, respectively. J is the electronic exchange coupling between the bridge and each metal basis state.

We shall use the present HFS-DVM transition operator results to calculate the parameters α and J contained in $\hat{H}_e$. First we simply diagonalize eq 6 to obtain three Hückel-type MO eigenvalues E_1, E_2, and E_3 in terms of α and J. Three transition energies, representing the three possible transitions between these MO's and written as $(E_3 - E_2)$, $(E_2 - E_1)$, and $(E_3 - E_1)$, are then calculated by using the transition operator method. These numerical energies are then equated with their corresponding expressions for the energy gaps obtained by diagonalizing eq 6. In this way, the many-electron HFS-DVM problem containing hundreds of basis states may be used to obtain an effective 3×3 electronic Hamiltonian. Since the present calculation is a spin-polarized one, this process is performed once for the spin up ↑ electrons and again for the spin down ↓ electrons.

Table VII. Values for the Parameters in $\hat{H}_{el}$ (in eV)

	from present calculation		
	spin up ↑ electrons	spin down ↓ electrons	from exptl data
α	1.7	0.93	1.4
J	−0.86	−0.85	−0.94

Values for α and J obtained for the C–T ion are given in Table VII. Note that the calculated values for the metal-to-bridge electron exchange coupling are the same (within reasonable bounds for error) for the spin up and spin down electrons (−0.86 and −0.85 eV, respectively). On the other hand, the value for α, the bridge-metal energy gap between the parent states, is significantly different for the spin up and spin down electrons (1.7 and 0.93 eV, respectively). This is due to spin–spin exchange splitting. The "experimental" values for α and J were obtained in the following manner: the expressions for the energy gaps in terms of α and J were equated with the observed energy maxima of the bonding-to-nonbonding and the nonbonding-to-antibonding transitions. Therefore the "experimental" values contain some vibronic effects (since the frequency maxima will be at least slightly shifted by vibronic interactions) and also do not distinguish between the spin states. (If the B → N transition is regarded as a transition by a spin down ↓ electron, then the N → A transition may be regarded as one by a spin up ↑ electron.) Thus, the "experimental" values for α and J do not provide direct information about the purely electronic part of the Hamiltonian for electrons of a given spin but do give us some guidance about the sizes of these two parameters.

In the next paper,[22] we shall show how these parameters may be used to predict the line shapes of OA transitions.

VII. A Model for the EPR g Tensor—Calculation of Hamiltonian Parameters

In an earlier paper[15] we presented a model for predicting the EPR g tensor of bridged mixed-valence dimers, with application to the Creutz–Taube ion. The model Hamiltonian is given by

$$\hat{H}_{eff} = \hat{H}_{cov} + \sum_k (\hat{H}^k_{tet} + \hat{H}^k_{rho} + \hat{H}^k_{so}) \tag{7}$$

$$\hat{H}_{cov} = \sum_\mu \alpha |\pi^{*\mu}\rangle\langle\pi^{*\mu}| + \sum_k \sum_\mu J\{|xz^\mu_k\rangle\langle\pi^{*\mu}| + |\pi^{*\mu}\rangle\langle xz^\mu_k|\} \tag{8}$$

$$\hat{H}^k_{tet} = \frac{D}{3}\left(\hat{L}_z^2 - \frac{1}{3}L(L+1)\right)_k \tag{9}$$

$$\hat{H}^k_{rho} = \frac{E}{12}(\hat{L}_+^2 + \hat{L}_-^2)_k \tag{10}$$

$$\hat{H}^k_{so} = \xi\left(\hat{L}_z\hat{S}_z + \frac{1}{2}\hat{L}_+\hat{S}_- + \frac{1}{2}\hat{L}_-\hat{S}_+\right)_k \tag{11}$$

where $\hat{H}_{cov}$ takes into account the strong coupling between one π^* state on the bridging ligand and the $4d_{xz}$ orbitals on the two metal ions. J is again the coupling constant for this interaction, and α is the energy gap between the parent π^* state and the parent $4d_{xz}$ orbitals. μ is the spin index (+ or −) and k (= L or R) labels the left and right metal-ion orbitals. D is the tetragonal splitting, E the rhombic splitting, and ξ the spin-orbit coupling.

In ref 15, we applied this model to the Creutz–Taube ion and successfully calculated the components of the anisotropic EPR g tensor. We now present the details of how the model Hamiltonian parameters were obtained from our electronic structure calculation.

Unlike OA energies, the EPR g tensor is a property of the electronic ground state only. Therefore, the parameters α and J for the EPR g tensor problem were obtained in the same manner

as for the OA line shape problem discussed above, except that ground-state energy gaps (between the A and N molecular orbitals, between N and B, and between A and B) were used in lieu of transition-state energy gaps. Again these values for the energy gaps are equated with the expressions for the Hückel energy gaps. Four of the resulting equations may be used to solve for α, J, D and E; the fifth provides a check. For the C–T ion, we obtained the values α = 1.2 eV and J = −0.79 eV (average for spin up ↑ and spin down ↓ electrons).

Because of the bridging ligand, each metal ion in a bridged dimer possesses lower than octahedral symmetry, which lifts the degeneracy of the metal t_{2g} d orbitals. Two of the five above-mentioned equations take the tetragonal and rhombic splittings into account. The five equations are given by

$$U_B = -x/2 + \alpha/2 - \tfrac{1}{2}[(\alpha + x)^2 + 8J^2]^{1/2} \quad (12)$$

$$U_N = -x \quad (13)$$

$$U_A = -x/2 + \alpha/2 + \tfrac{1}{2}[(\alpha + x)^2 + 8J^2]^{1/2} \quad (14)$$

$$U_{x^2-y^2} = \tfrac{2}{3}D \quad (15)$$

$$U_{yz} = -\tfrac{1}{3}D + \tfrac{1}{2}E \quad (16)$$

where $x = {}^1/_3D + {}^1/_2E$ and where the U's are the ground state MO energies of the Ru 4d orbitals.

Equation 11 takes into account the spin-orbit coupling, a feature missing from the present nonrelativistic HFS-DVM calculation. The manifestations of spin-orbit coupling in the electronic spectra are discussed in the next section. By using the fitted value for the spin-orbit coupling ζ = 0.087 eV, we obtain the g tensor components as g_{xx} = 1.36, g_{yy} = 2.85, and g_{zz} = 2.45, which are in agreement with experiment to within 1–2%.[15]

VIII. Some Further Thoughts on Transition Assignments

In section V we discussed the assignments of some of the electronic transitions observed for the C–T ion, utilizing the transition operator method. We also pointed out that there are some observed transitions which could not be assigned by this method alone. The simple seven state model discussed in the preceding section builds the effects of spin-orbit coupling into the problem. Therefore this simple model is capable of predicting some transitions which the transition operator method cannot. One should remember however that this simple model was designed to predict properties of the electronic ground state. We have used ground-state Hamiltonian parameters and this introduces errors into the transition energies calculated from differences between the energy eigenvalues. Thus transition energies calculated by this method are only approximate.

Predicted transition energies, assignments, and transition polarizations are given in the right hand columns of Table VI.

Note that the transition energies predicted by this method tend to be too low by 15–20% and only qualitative at very low energies. The simple model predicts two transitions corresponding to $t_{2g} \rightarrow A$ at 17 000 and 16 000 cm^{-1}. These two transitions both have two components, one x-polarized and one z-polarized. Tentatively, we assign the two MCD features at 20 400 and 17 400 cm^{-1} to these two transitions. The simple model also places the nonbonding-to-antibonding transition (z-polarized) at 15 000 cm^{-1}. In the OA spectrum, these three transitions appear as a broad, unresolved band with frequency maximum at about 18 000 cm^{-1}.

The IT (B → N) transition was predicted to occur at 5700 cm^{-1}. As one would expect, the transition operator prediction was much closer to the observed frequency maximum of 6400 cm^{-1}.

We were able to assign tentatively the two MCD features at 4000 and 2000 cm^{-1} to $4d_{yz}$-to-nonbonding and $4d_{x^2-y^2}$-to-nonbonding transitions.

The seven state model was not able to account for the MCD feature at 12 800 cm^{-1} nor for the weak shoulder seen in the OA spectrum at about 12 000 cm^{-1}.

IX. Conclusions

Our HFS-DVM results show strong mixing of the two Ru $4d_{xz}$ orbitals with one π^* orbitals in the Creutz–Taube ion, with the two Ru ions equivalent. When the bond lengths are changed from the symmetric crystallographic geometry to a plausible asymmetric geometry, the Ru ions are still extensively mixed via the π^* orbital and the Mulliken charges of the two Ru ions are very nearly identical. This is evidence for a delocalized ground state.

Our transition operator calculations have confirmed the original[2,3] assignments of the OA transitions at 252, 565, and 1570 nm.

Our transition operator calculations together with our simple seven state model account for nearly all of the observed OA and MCD features. The seven state model, which incorporates spin-orbital coupling, complements the inherently more accurate transition operator work because it can predict transitions which are beyond the scope of the nonrelativistic HFS-DVM calculations. We have made predictions about the polarizations of the components of the band observed in the OA at about 18 000 cm^{-1}. In the next paper, we shall discuss the line shape of the z-polarized part of this transition. We hope that this energy region will be studied by single-crystal polarized spectra.

Neither the transition operator method nor the simple seven state model is able to account for the MCD feature at 12 800 cm^{-1} nor for the weak shoulder seen in the OA at 12 000 cm^{-1}. Possibly these could arise from a doublet → quartet transition.[9]

We have shown how the results of the HFS-DVM calculation may be used to obtain the Hamiltonian parameters (except for the spin-orbit coupling) needed to predict the components of the EPR g tensor. Ours is the only treatment to date which not only correctly calculates the g tensor components but also places several observed electronic transitions at approximately the right energies. Ours also uses the fewest number of arbitrary parameters to date (i.e., one: the spin-orbit coupling).

We have shown how the transition operator results may be used to obtain values for the electronic Hamiltonian parameters needed for the OA line shape problem. Applications to the OA line shape[17,26] of the CT ion are discussed in the next paper.[22]

Acknowledgment is made to the National Science Foundation for support of this research under Grant No. CHE 8607693 and to the donors of the Petroleum Research Fund, administered by the American Chemical Society. We thank the Arthur D. Little Foundation for an Arthur D. Little Fellowship awarded to Jaeju Ko. We are grateful to Professor Bengt Lindgren for a copy of his HFS-DVM program. We thank Professors D. E. Ellis and M. A. Ratner for many useful discussions. M.J.O. acknowledges the support of the Danish Natural Science Research Council and the hospitality of Professor Jan Linderberg during her stay at Aarhus Universitet.

Registry No. $[(NH_3)_5Ru(pyz)Ru(NH_3)_5]^{5+}$, 35599-57-6.

(26) Ko, J. Ph.D. Dissertation, Northeastern University, 1986.